Cytokine 166 (2023) 156187

Contents lists available at ScienceDirect

Cytokine

journal homepage: www.elsevier.com/locate/cytokine

Identification of key differentially expressed genes in SARS-CoV-2 using RNA-seq analysis with a systems biology approach

Arash Safarzadeh [a], Bashdar Mahmud Hussen [b], Mohammad Taheri [c,d,*], Soudeh Ghafouri-Fard [a,*], Mohammadreza Hajiesmaeili [e,*]

[a] Department of Medical Genetics, School of Medicine, Shahid Beheshti University of Medical Sciences, Tehran, Iran
[b] Department of Clinical Analysis, College of Pharmacy, Hawler Medical University, Kurdistan Region, Erbil, Iraq
[c] Urology and Nephrology Research Center, Shahid Beheshti University of Medical Sciences, Tehran, Iran
[d] Institute of Human Genetics, Jena University Hospital, Jena, Germany
[e] Anesthesia and Critical Care Department, Critical Care Quality Improvement Research Center, Loghman Hakim Hospital, Shahid Beheshti University of Medical Sciences, Tehran, Iran

ARTICLE INFO

Keywords:
SARS-CoV-2
Gene expression
Immune response

ABSTRACT

COVID-19 is associated with dysregulation of several genes and signaling pathways. Based on the importance of expression profiling in identification of the pathogenesis of COVID-19 and proposing novel therapies for this disorder, we have employed an *in silico* approach to find differentially expressed genes between COVID-19 patients and healthy controls and their relevance with cellular functions and signaling pathways. We obtained 630 DEmRNAs, including 486 down-regulated DEGs (such as CCL3 and RSAD2) and 144 up-regulated DEGs (such as RHO and IQCA1L), and 15 DElncRNAs, including 9 down-regulated DElncRNAs (such as PELATON and LINC01506) and 6 up-regulated DElncRNAs (such as AJUBA-DT and FALEC). The PPI network of DEGs showed the presence of a number immune-related genes such as those coding for HLA molecules and interferon regulatory factors. Taken together, these results highlight the importance of immune-related genes and pathways in the pathogenesis of COVID-19 and suggest novel targets for treatment of this disorder.

1. Introduction

COVID-19 caused by SARS-CoV-2 has produced a pandemic with heavy burden on health system all over of the world. Several investigations have been conducted to unravel the signaling pathways and gene expression patterns altered by this virus [1,2]. These studies would help in identification of the molecular mechanisms responsible for high mortality of this disorder and finding suitable markers for prediction of course of COVID-19. For instance, whole transcriptome analyses have revealed up-regulation of neutrophil-related transcripts and down-regulation of T cell related transcripts in SARS-CoV2-affected persons, particularly severely affected ones [3]. Moreover, single-cell and bulk RNA sequencing assays in these patients have revealed inflammatory mechanisms for COVID-19-associated organ damage [4]. In addition, a comprehensive assessment of transcriptome of organs affected by this virus has indicated the role of a group of myeloid-lineage cells with extremely inflammatory but distinctive expression profile in each part in the pathogenesis of COVID-19-related complications [5]. Based on this data, transcriptomic profiling has been suggested as a tool for identification of the pathogenesis of COVID-19 in each affected individual [5].

Based on the importance of expression profiling investigations in identification of the pathogenesis of COVID-19 and proposing novel therapies for this disorder, we have employed an *in silico* approach to discover differentially expressed genes between COVID-19 patients and healthy controls and their relevance with cellular functions and signaling pathways.

2. Methods

2.1. Collection of RNA-seq data and evaluation of dataset quality

In order to acquire the RNA-seq raw counts of GSE184610 (Illumina NovaSeq 6000 (Homo sapiens); GPL24676), we utilized the Gene Expression Omnibus (GEO; https://www.ncbi.nlm.nih.gov/geo/). A total of 138 negative control samples and 204 SARS-CoV-2 positive patient mucosa samples were chosen for further analysis. In Rstudio

* Corresponding authors.
E-mail addresses: Mohammad.taheri@uni-jena.de (M. Taheri), S.ghafourifard@sbmu.ac.ir (S. Ghafouri-Fard), mrhajiesmaeili@sbmu.ac.ir (M. Hajiesmaeili).

https://doi.org/10.1016/j.cyto.2023.156187
Received 6 November 2022; Received in revised form 31 January 2023; Accepted 14 March 2023
Available online 24 March 2023

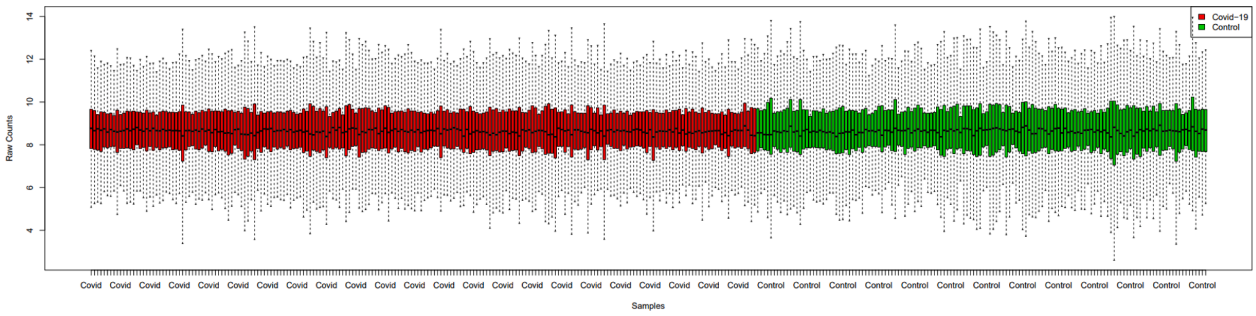

Fig. 1. Boxplot of normalized counts. The median between the samples is not significantly different, according to this box plot.

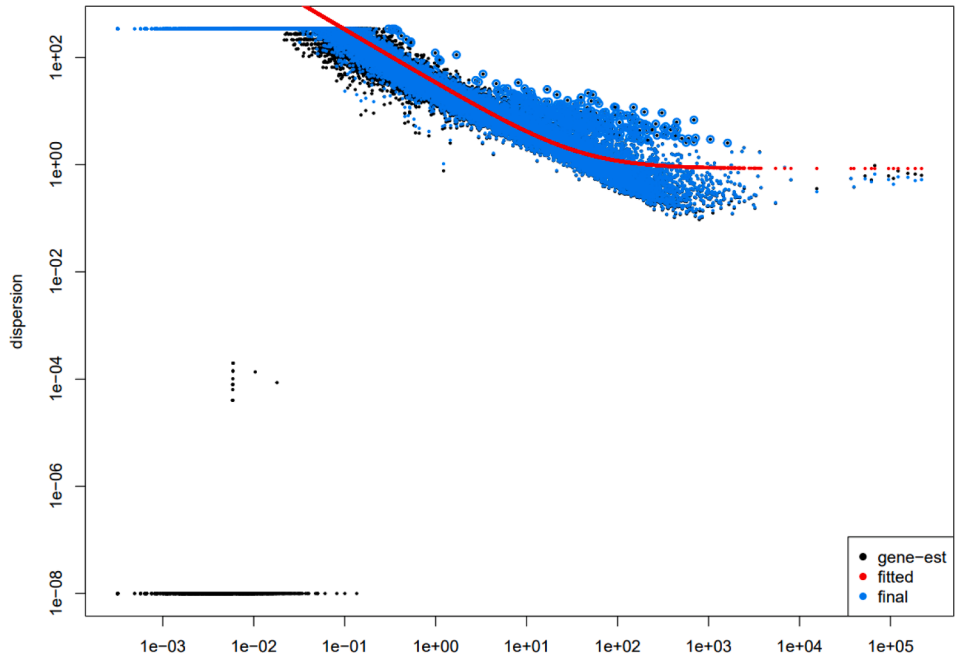

Fig. 2. Dispersion estimate plot. Gene-wise estimates, the fitted values and the final maximum a posteriori estimates used in testing are shown in black, red and blue, respectively.

software (version 4.0.4), we imported the dataset and assessed its quality. This step involves investigating raw counts and normalized counts boxplots and investigating dispersion estimate plot.

2.2. The dataset preprocessing and DEGs analysis

We analyzed raw counts data using DESeq2 package [6] and got DEGs using lfcShrink function via normal method. In addition, Bonferroni was used to adjust the P value into the FDR. We used the FDR <0.05 and $|\log2\ FC| > 1$ as the cutoff criteria for DEmRNAs and DElncRNAs.

2.3. Gene ontology (GO) enrichment analyses

We used the clusterProfiler R package [7] to accomplish Gene Ontology (GO) enrichment analyses to explore the function of the identified up-regulated and down-regulated DEmRNAs. The functional category criteria were established at an adjusted p-value of 0.05 or below.

2.4. Kyoto encyclopedia of genes and genomes (KEGG) pathway analysis

To determine the probable roles of these genes, KEGG pathway analysis [8] of significantly up-regulated and down-regulated DEGs was performed.

2.5. PPI network construction and hub genes identification

The PPI network for DEGs was built using the STRING database [9]. The interactions parameter was established using the highest level of confidence (confidence score >0.9). The interactions between the proteins were shown using Cytoscape software version 3.9 [10]. The Cytohubba plugin of Cytoscape [11] and the degree method were finally used to identify the top 20 DEGs associated with hub genes.

2.6. Receiver operating characteristic (ROC) curve analysis

The area under the curve (AUC) values derived from receiver operating characteristic (ROC) curve analysis were used to assess the diagnostic efficacy of hub genes.

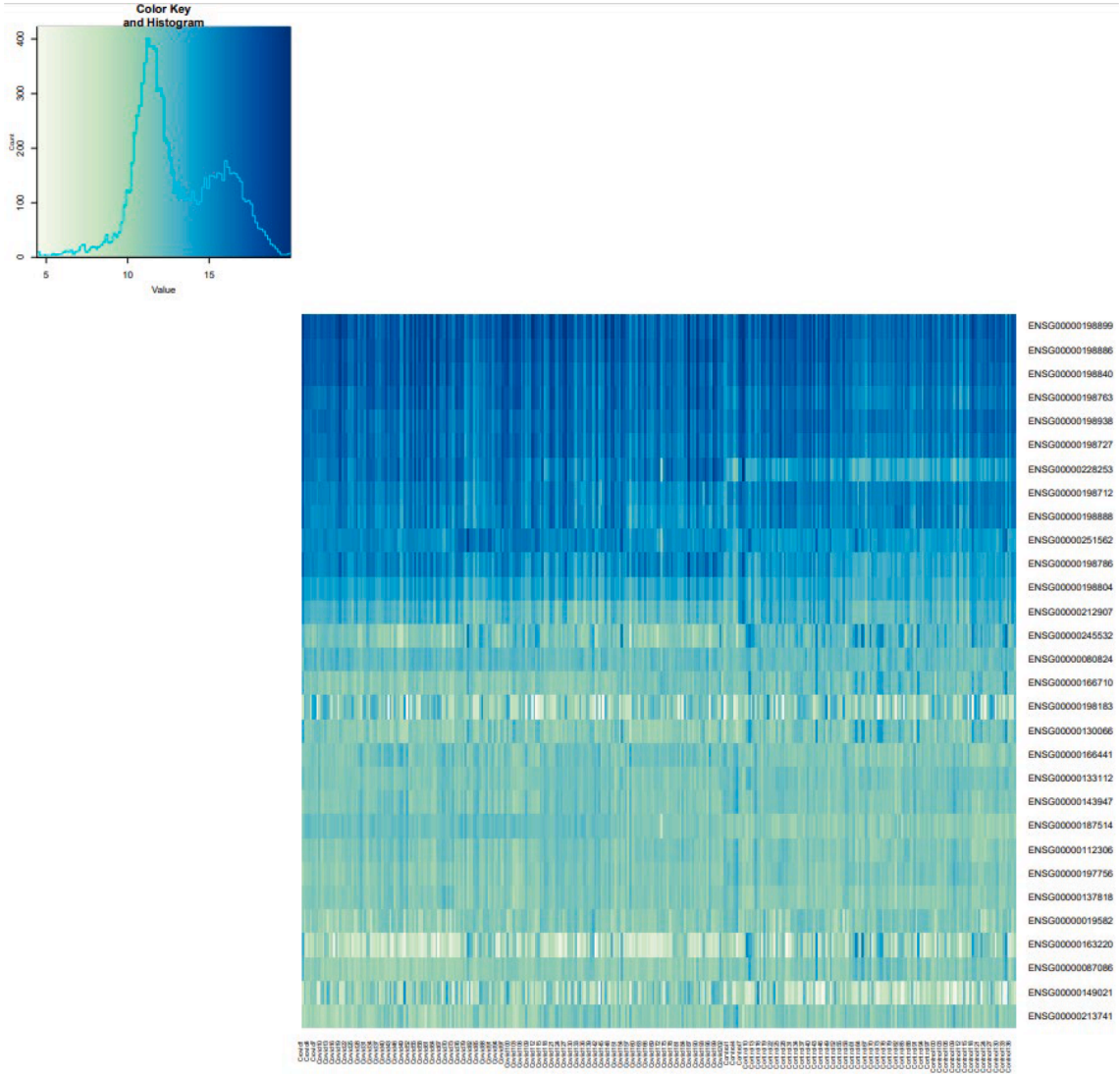

Fig. 3. The 30 most highly expressed genes' expression data shown as heatmap.

Table 1
The top 10 up- and down-regulated DEmRNAs between SARS-CoV-2 positive patient mucosa and negative control samples.

Down-regulated			Up-regulated		
DEmRNA	Log FC	Adjusted *P* value	DEmRNA	Log FC	Adjusted P value
CCL3	−3.522198	6.05904939329508e−05	RHO	5.999073	5.06593453378896e−58
RSAD2	−3.277750	3.53839507223347e−17	IQCA1L	2.755854	1.79906859343439e−05
PLAU	−3.268583	2.8779631834047e−05	CCDC168	2.638627	1.46038298795042e−05
CCL2	−3.256825	4.22788513280451e−06	FILIP1L	2.582805	1.08123055561509e−05
CCL4	−3.248852	1.83460110250716e−07	PKD1L3	2.572879	2.72911233018633e−15
IFIT3	−3.219601	7.64206271929218e−23	ND6	2.422819	5.06593453378896e−58
FCER1G	−3.173030	5.47213646256583e−27	KCNJ6	2.402090	0.000189331612680773
IFITM1	−3.167388	3.64641305252621e−21	L1TD1	2.388298	2.34425812741455e−06
C3AR1	−3.157713	1.53267505111211e−09	ARC	2.341139	9.09298952655054e−05
TNFAIP6	−3.015891	1.26235650172001e−08	MUCL3	2.251693	0.000454333529852898

Table 2
The significantly up- and down-regulated DElncRNAs between SARS-CoV-2 positive patient mucosa and negative control samples.

Down-regulated			Up-regulated		
DElncRNA	Log FC	Adjusted *P* value	DElncRNA	Log FC	Adjusted P value
PELATON	−2.414951	4.70603855680276e-06	AJUBA-DT	1.891883	0.00145743231643265
LINC01506	−2.189435	0.000276966532762493	FALEC	1.861288	0.0277160449944691
MIR223HG	−1.776585	0.0136203042254115	MZF1-AS1	1.834784	1.69156430996055e-05
FTX	−1.672565	0.00233406934840649	RNF139-DT	1.653451	0.00229169343117678
ATP2B1-AS1	−1.514810	0.00521350099762486	LMO7DN	1.375112	0.00377205696800783
NEAT1	−1.343839	6.71027975173219e-07	SNHG31	1.314847	0.0394361017036223
CYTOR	−1.289805	0.0105166377130368			
NUP50-DT	−1.222082	0.00826370673115181			
MIR4435-2HG	−1.040226	0.0359620111847791			

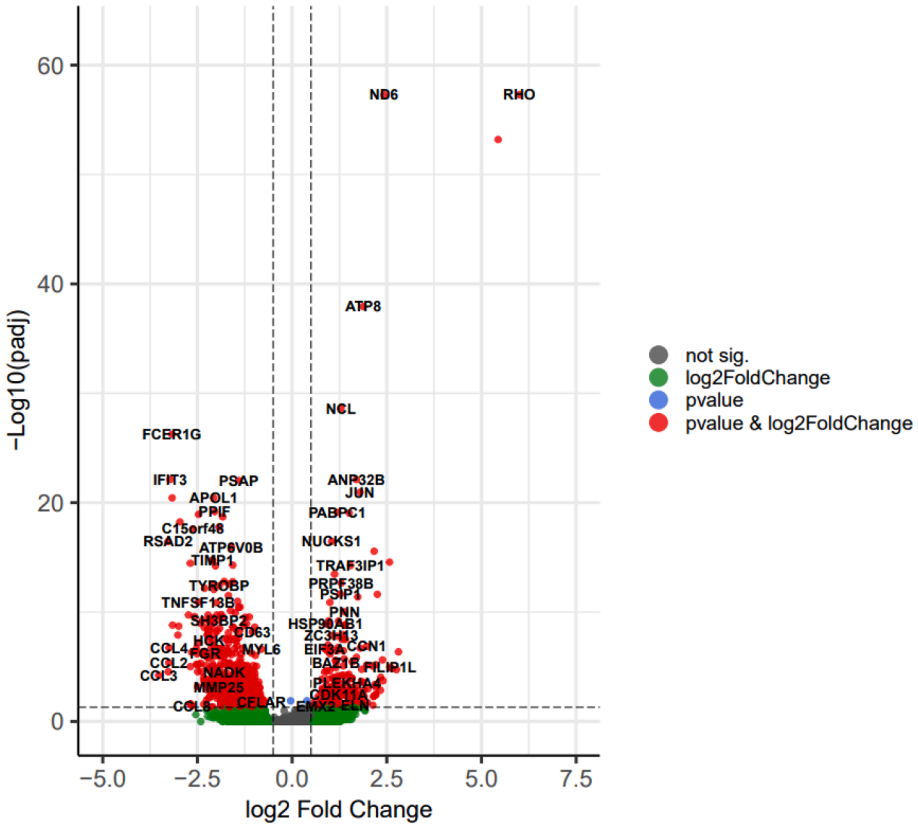

Fig. 4. The volcano plot of differentially expressed genes (DEGs); horizontal axis, log2(FC); vertical axis, -$\log_{10}$(adjusted P value).

2.7. Regulatory network of miRNA-hub genes and TF-hub genes

Finally, the Networkanalyst database [12] was used to create the relationships between the hub genes and the transcription factors (TFs) and microRNAs (miRNAs).

3. Results

3.1. Dataset quality assessment

To normalize the raw counts, we utilized the DESeq2 package and the normalized counts transformation method. The boxplot of the normalized data for each sample is shown in Fig. 1. This boxplot shows that the data quality was acceptable. The dispersion estimate plot (Fig. 2) displays the gene-wise estimates, the fitted values, and the final maximum a posteriori estimates used in testing. This graphic demonstrates that the DESeq2 model fits the data well. Heatmap of the count Table is shown in Fig. 3. In this figure, we used variance stabilizing transformation (VST) method to show the heatmap of top 30 genes.

3.2. DEGs analysis

Based on the RNA-seq data analysis between SARS-CoV-2 positive and control samples by DESeq2 package, we obtained 630 DEmRNAs, including 486 down-regulated DEGs (such as CCL3 and RSAD2) and 144 up-regulated DEGs (such as RHO and IQCA1L), and 15 DElncRNAs, including 9 down-regulated DElncRNAs (such as PELATON and LINC01506) and 6 up-regulated DElncRNAs (such as AJUBA-DT and FALEC). Table 1 lists the top 10 down-regulated and up-regulated DEmRNAs. Table 2 lists down-regulated and up-regulated DElncRNAs.

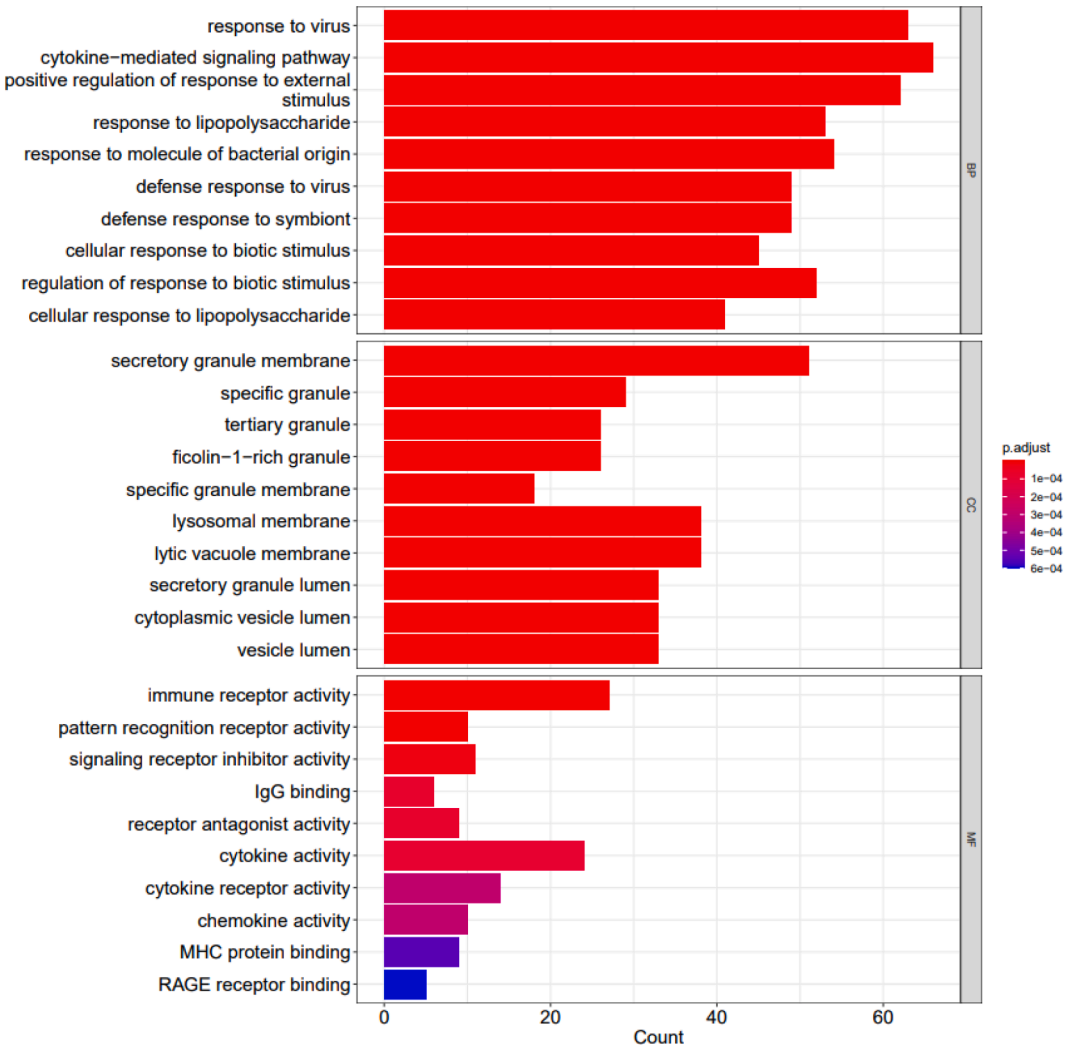

Fig. 5. The barplots of top 10 enriched functions; BP (biological process), CC (cellular component) and MF (molecular function). X axis shows the count of geneset; Y axis shows the geneset function; Bar color represents the adjusted P.value, ranging from red (most significant) to blue (least significant).

The variations of lncRNA and mRNA expression between SARS-CoV-2 positive patient mucosa and negative control samples were visualized and assessed using volcano plot (Fig. 4).

3.3. GO enrichment analysis of DEGs

In this study, the considerably DEGs were enriched in 774 GO terms. We used Clusterprofiler package to perform analysis. In GO functional enrichment analysis, 774 GO entries satisfy Adjusted P value less than 0.05, most of which are biological processes (BP), followed by cellular component (CC) and molecular function (MF). The first 30 entries are response to virus (BP), cytokine-mediated signaling pathway (BP), positive regulation of response to external stimulus (BP), secretory granule membrane (CC), response to lipopolysaccharide (BP), response to molecule of bacterial origin (BP), defense response to virus (BP), defense response to symbiont (BP), cellular response to biotic stimulus (BP), regulation of response to biotic stimulus (BP), cellular response to lipopolysaccharide (BP), cellular response to molecule of bacterial origin (BP), positive regulation of cytokine production (BP), leukocyte chemotaxis (BP), leukocyte migration (BP), myeloid leukocyte migration (BP), negative regulation of viral genome replication (BP), regulation of innate immune response (BP), immune response-regulating signaling pathway (BP), granulocyte migration (BP), pattern recognition receptor signaling pathway (BP), cell chemotaxis (BP), positive regulation of defense response (BP), neutrophil migration (BP), leukocyte mediated immunity (BP), regulation of viral genome replication (BP), negative regulation of immune system process (BP), myeloid leukocyte activation (BP), viral genome replication (BP) and neutrophil chemotaxis (MF). As a result, the majority of the terms are related to the immune system and the body's viral defense system. In this way, the outcomes support the GO enrichment analysis. Fig. 5 shows the barplots of top 10 enriched functions.

Figs. 6 and 7 depict visualization of the dotplots of top 10 enriched functions and enriched GO induced graph, respectively.

In Fig. 8, the UpSet plot visualizes the intersection between top 10 GO terms. It highlights the gene overlap between several gene sets.

Fig. 9 indicates the gene-concept network of top 5 GO terms (cytokine-mediated signaling pathway, positive regulation of response to external stimuli, response to polysaccharides, response to molecules of bacterial origin and response to virus).

3.4. Pathway analysis

Using Pathview [13] and gage [14] packages in R, KEGG pathways analysis [15,16] of 486 down-regulated and 144 up-regulated DEmRNAs were performed to identify the potential functional genes (Fig. 10).

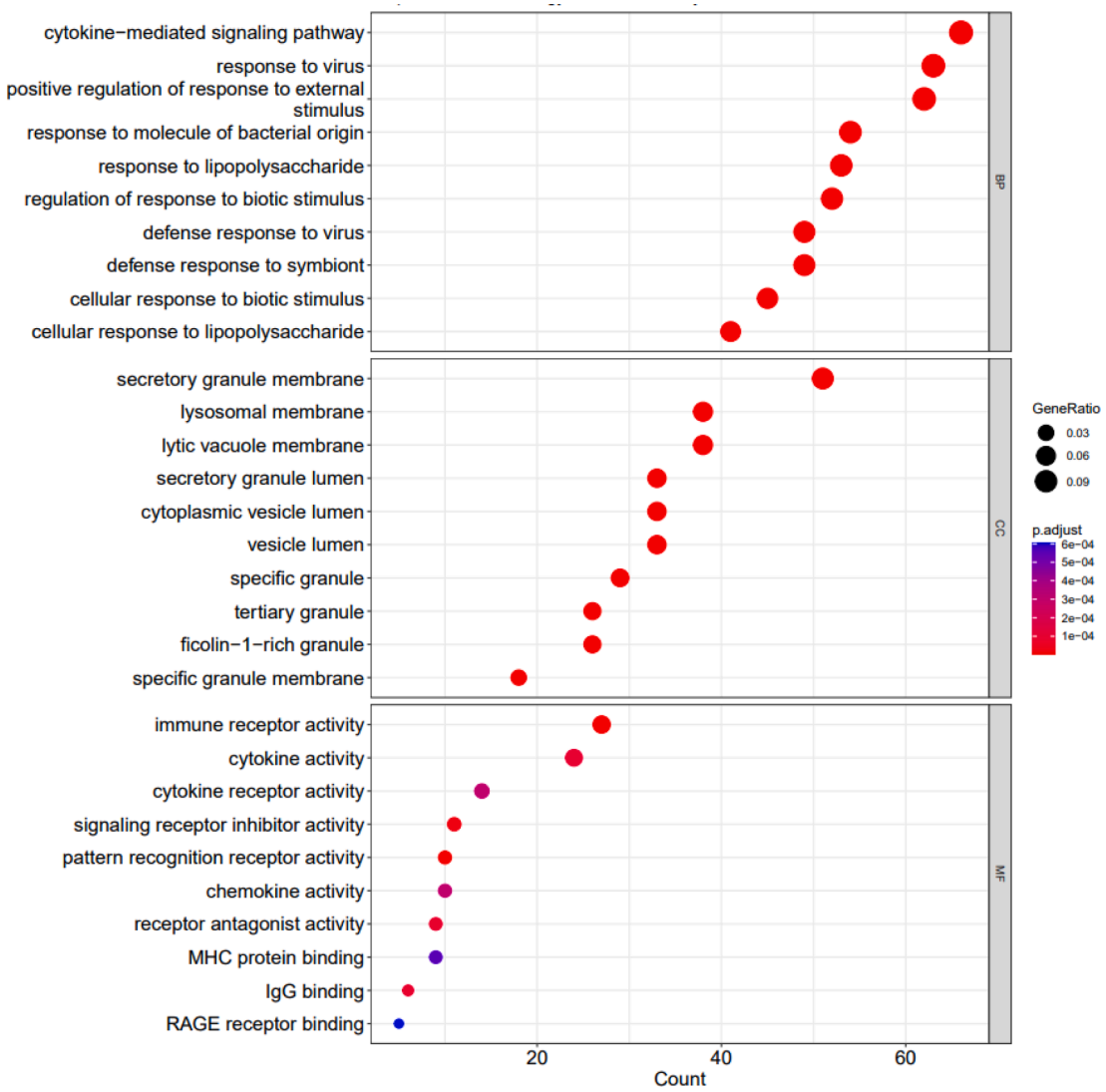

Fig. 6. The dotplots of top 10 enriched functions. X axis shows the count of geneset; Y axis shows the geneset function; Dot color represents the adjusted P value ranging from dark blue (most significant) to red (least significant). Dot size represents the GeneRatio and the larger the size of the dot, the higher the value of the gene ratio.

Downregulated pathways are listed in Table 3 and Fig. 10. Pathways were related to immune system functions in a manner similar to what we saw in the gene ontology terms.

3.5. PPI network construction and selection of hub genes

A PPI network of DEGs (Fig. 11) with 204 nodes and 590 edges that was generated from STRING was put into the Cytohubba plugin of Cytoscape 3.9 to recognize the hub genes. The 20 hub genes with the highest degree of connectivity were HLA-A, IRF7, STAT2, ISG20, IFI6, XAF1, IFIT5, IFIT3, IFIT2, HLA-C, RSAD2, IFITM2, IFI35, IFITM3, IFITM1, HLA-B, MX2, MX1, IFIT1 and ISG15 (Table 4).

3.6. Validation of hub genes

We used graphpad prism 9.0 to construct ROC curves. The accuracy of the hub genes predictions was assessed using the ROC curve. The diagnostic values of these hub genes were compared using AUC. ROC curves and AUC values of dataset are shown in Fig. 12. The computed AUC values in this study varied from 0.7 to 1, which is considered to have high discriminative power. According to the ROC analysis, the expression levels of 9 hub genes showed high diagnostic value.

3.7. Identification of the regulatory network of miRNA-hub genes

The Networkanalyst online database was used to collect miRNAs that target hub genes (Fig. 13). Hsa-miR-146a-5p and has-miR-29b-3p were regarded as significant miRNAs since they interacted with hub genes at the greatest level (degree 3) possible (Fig. 14).

3.8. Examination of the regulatory network of TF-hub genes

We obtained TFs targeting hub genes from the Networkanalyst database (Fig. 13). The TF-hub gene network showed that the SPI1 regulates six hub genes.

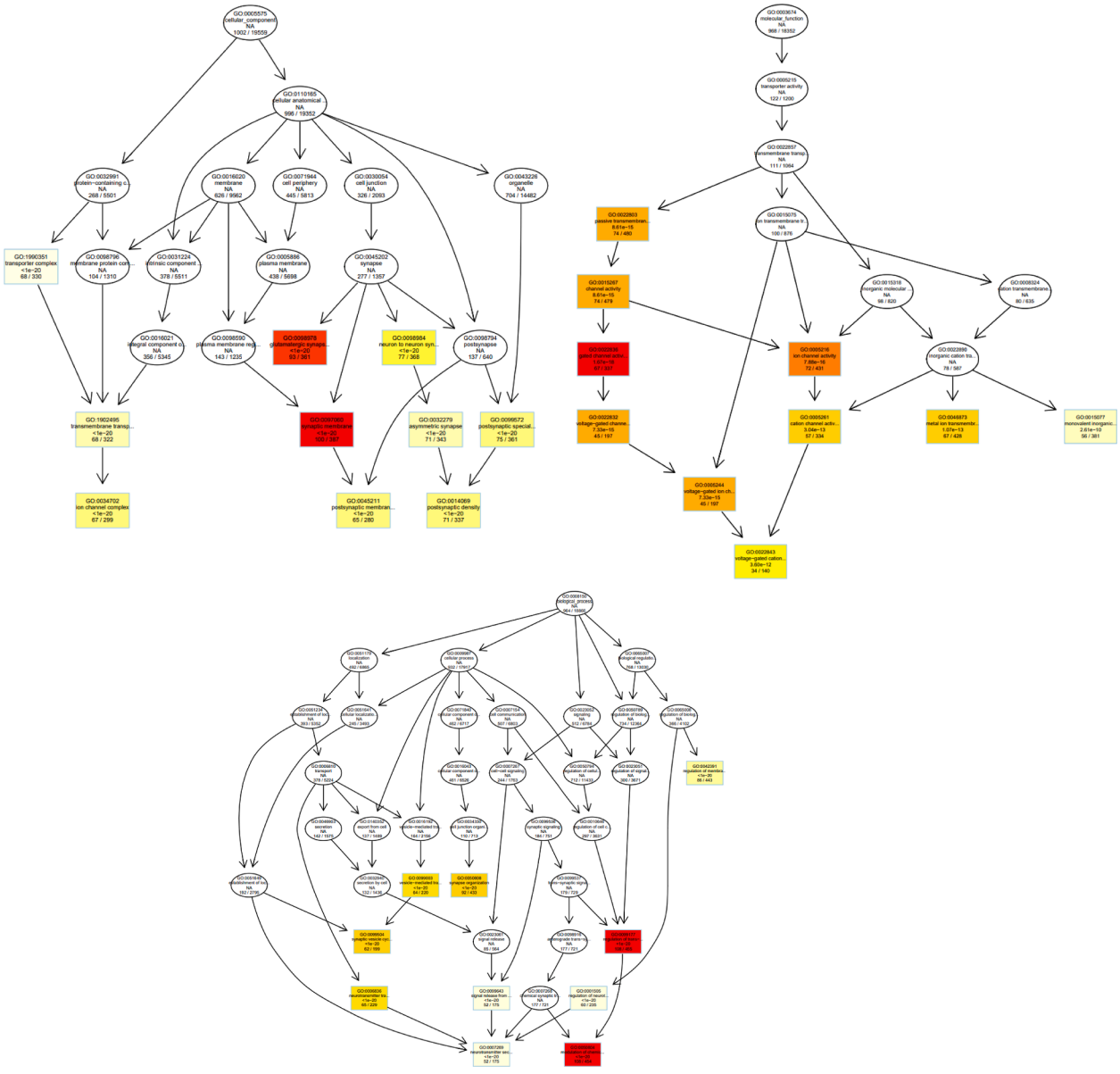

Fig. 7. GO graph visualization of top GO terms enriched. (A) The top 10 GO terms in the category "Cellular Component" have generated a GO sub-graph. (B) The top 10 GO terms in the category "Molecular Function" have generated a GO sub-graph. (C) The top 10 GO terms in the category "Biological process" have generated a GO sub-graph. Boxes indicate the most significant terms. From dark red (most significant) to light yellow (least significant), the color of the box indicates the relative significance.

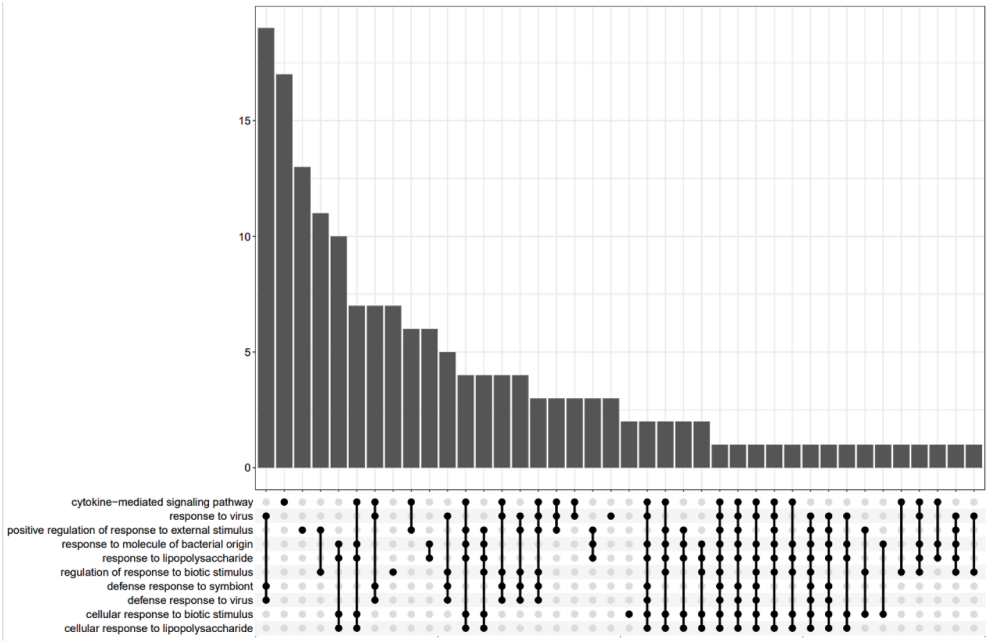

Fig. 8. UpSet plot of top 10 GO terms.

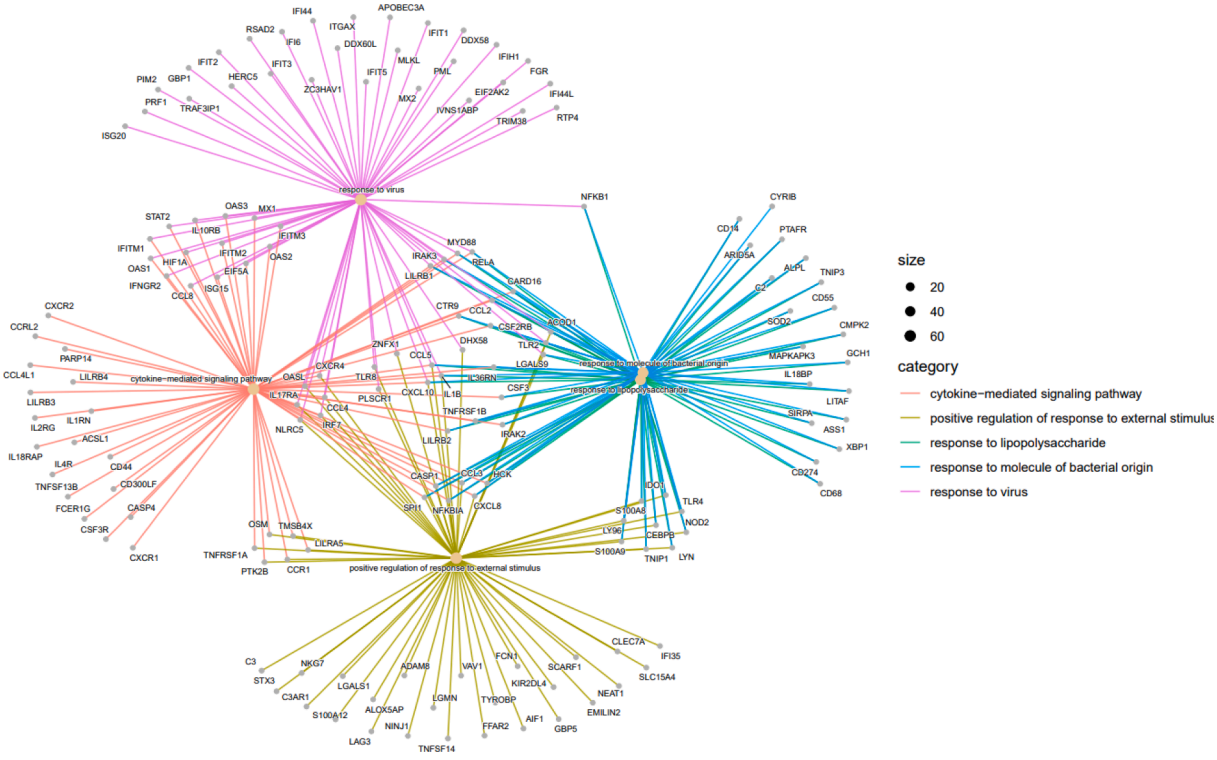

Fig. 9. Top 5 GO terms as a network plot. These GO terms were connected to genes in this graph. The connection of genes to the corresponding GO is marked with a special color. There are more genes for a specific GO term if the dot relating to it is bigger.

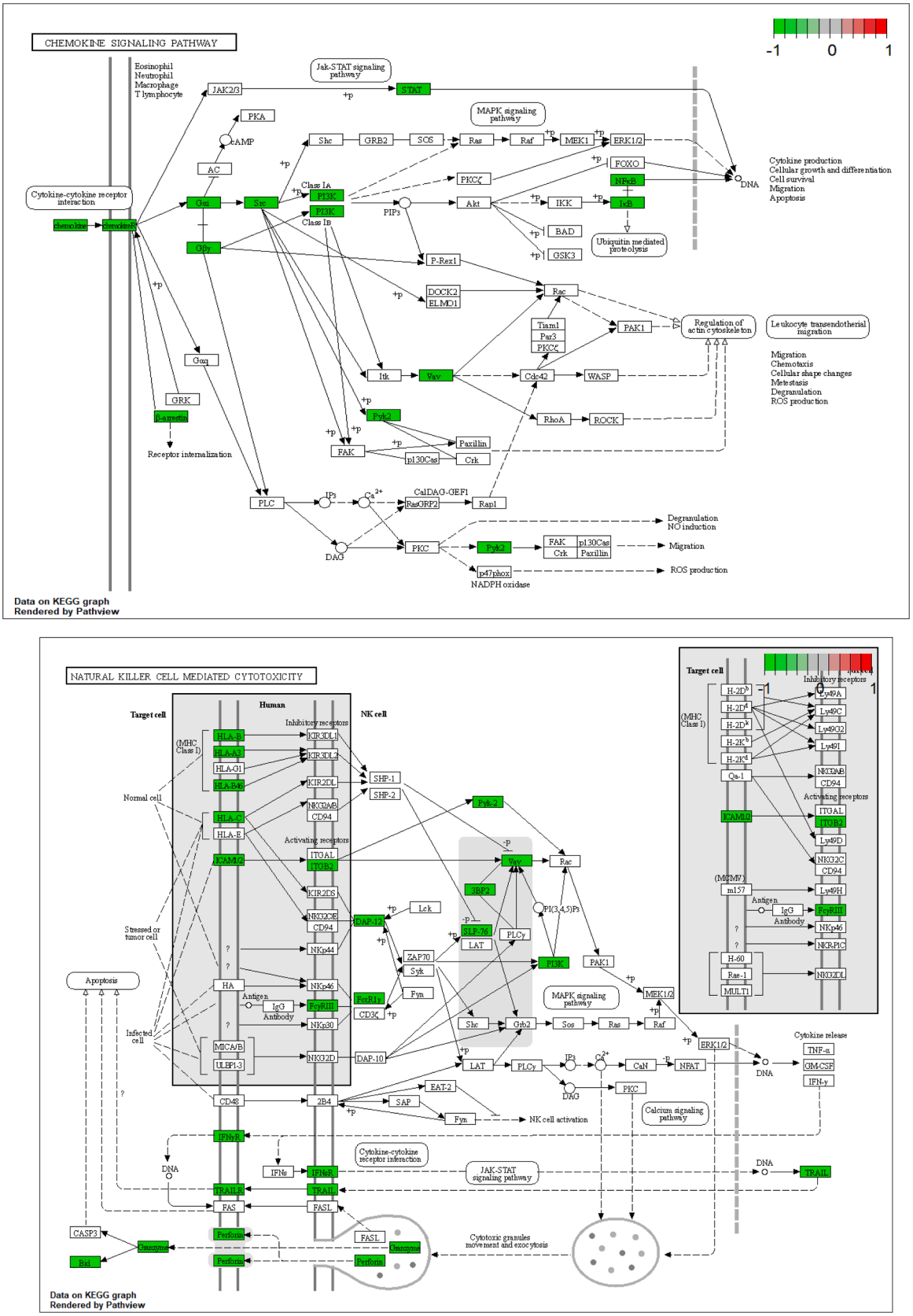

Fig. 10. Visualization of pathways. Green boxes are down-regulated genes and Red boxes are up-regulated genes.

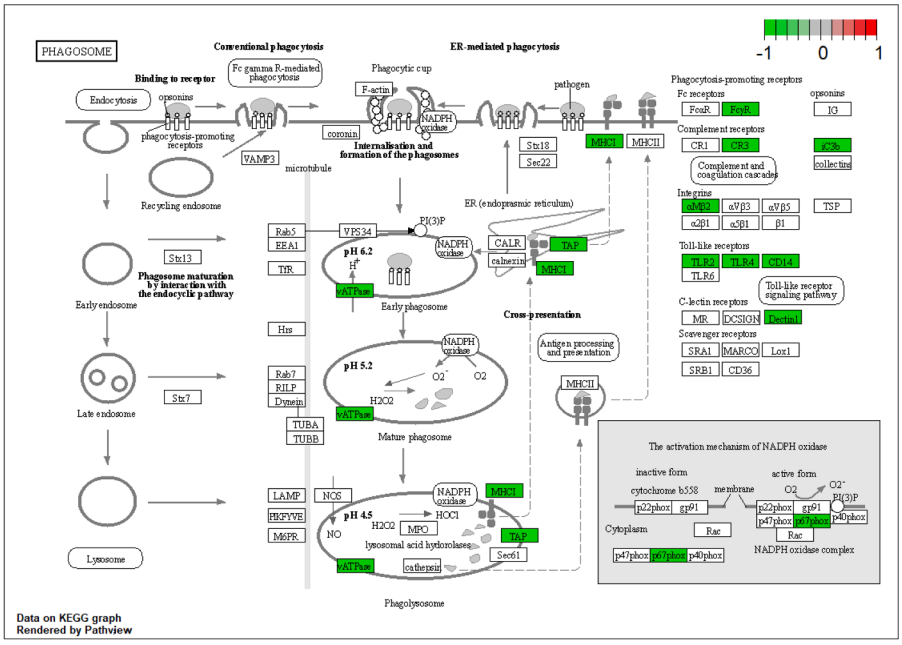

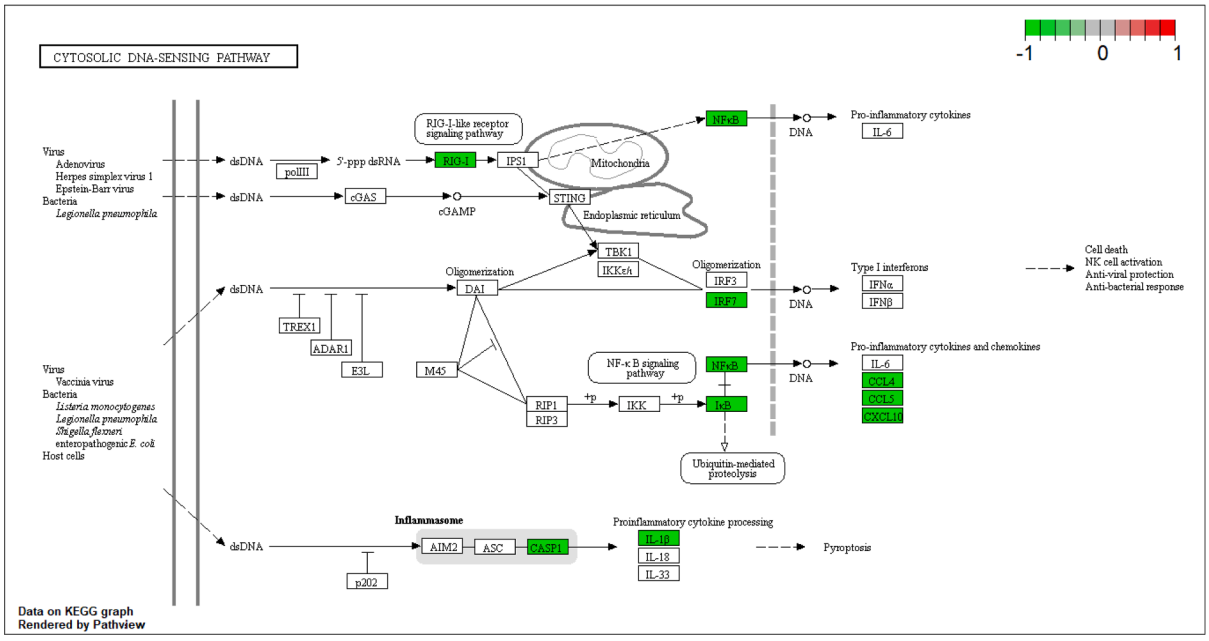

Fig. 10. (*continued*).

Table 3
Down- and up-regulated pathways.

Down-regulated		Up-regulated	
Pathway	P value	Pathway	P value
Chemokine signaling pathway	0.002948037	–	–
Natural killer cell mediated cytotoxicity	0.011685555		
Phagosome	0.020611266		
Cytosolic DNA-sensing pathway	0.038850553		

4. Discussion

COVID-19 has been shown to trigger strong alterations in the blood transcriptome. Most notably, recent studies have demonstrated associations between the severity of COVID-19 and remarkable alterations in the neutrophil- and T cell-related transcripts [3]. Expression of a variety of other transcripts has also been found to be altered in COVID-19 patients [1,2]. In the current investigation, we developed an *in silico* approach to find the most important altered genes and signaling pathways in COVID-19. Our analysis included both mRNAs and lncRNAs. CCL3, RSAD2, PLAU, CCL2, CCL4, IFIT3, FCER1G, IFITM1, C3AR1 and TNFAIP6 have been among the most significantly down-regulated mRNAs in COVID-19 patients. CCL3, CCL2 and CCL4 are among chemokines whose expressions are induced by IL-1 and TNF-α and are associated with viral infections [17]. C3AR1 is a receptor for C3a, an

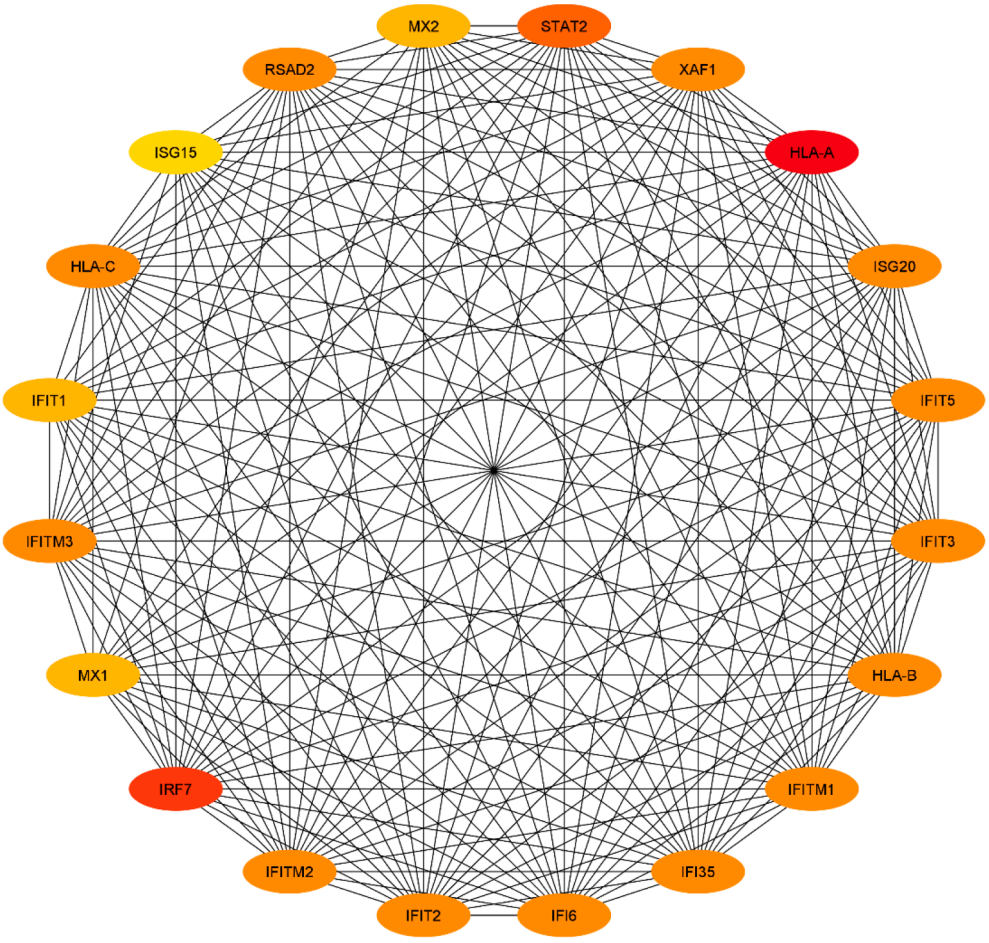

Fig. 11. PPI network of DEmRNAs.

Table 4
The information of hub genes in PPI network.

Hub Gene	Adjusted P.value	Log2FC	Clustering Coefficient	Degree	Closseness Centrality	Betweenness Centrality
HLA-A	1.17405388074575e−09	−1.2017269612983	0.5060483870967	32	0.33568075117370	0.12130993483553777
HLA-B	2.98101242818701e−10	−1.2397535042883	0.9525691699604	23	0.30232558139534	6.628294880535598E−5
HLA-C	3.69143414621164e−11	−1.4158897587374	0.9525691699604	23	0.30232558139534	6.628294880535598E−5
IFI35	0.00640167112233584	−1.2988153793527	0.9525691699604	23	0.30232558139534	6.628294880535598E−5
IFI6	3.01430541463456e−08	−1.6981280098013	0.9525691699604	23	0.30232558139534	6.628294880535598E−5
IFIT1	1.84638421809207e−10	−2.7365819306463	0.7965367965367	22	0.30555555555555	0.011495532937713914
IFIT2	8.79161316577004e−06	−2.0775489444141	0.9525691699604	23	0.30232558139534	6.628294880535598E−5
IFIT3	7.64206271929218e−23	−3.2196014206250	0.9525691699604	23	0.30232558139534	6.628294880535598E−5
IFIT5	0.00707778449749948	−1.4779750161670	0.9525691699604	23	0.30232558139534	6.628294880535598E−5
IFITM1	3.64641305252621e−21	−3.1673883849525	0.9525691699604	23	0.30232558139534	6.628294880535598E−5
IFITM2	8.44762880149889e−13	−2.0662886199984	0.9525691699604	23	0.30232558139534	6.628294880535598E−5
IFITM3	5.97268740910169e−15	−2.0245315549745	0.9525691699604	23	0.30232558139534	6.628294880535598E−5
IRF7	2.67513242124973e−09	−2.1167282760516	0.7538461538461	26	0.37434554973821	0.16382876903582366
ISG15	5.7319781821844e−19	−2.9625688389390	0.8761904761904	21	0.30296610169491	0.004010616268719467
ISG20	6.46627575844399e−08	−1.6804788202611	0.9525691699604	23	0.30232558139534	6.628294880535598E−5
MX1	7.48158579565845e−11	−1.6250252592217	0.7965367965367	22	0.30555555555555	0.011495532937713914
MX2	5.7837259618947e−07	−1.6739982781717	0.7965367965367	22	0.30555555555555	0.011495532937713914
RSAD2	3.53839507223347e−17	−3.2777509714946	0.9525691699604	23	0.30232558139534	6.628294880535598E−5
STAT2	1.28468555594202e−05	−1.4236338499166	0.8033333333333	25	0.32426303854875	0.03551181801181966
XAF1	0.000652170971128252	−1.2553337367898	0.9525691699604	23	0.30232558139534	6.628294880535598E−5

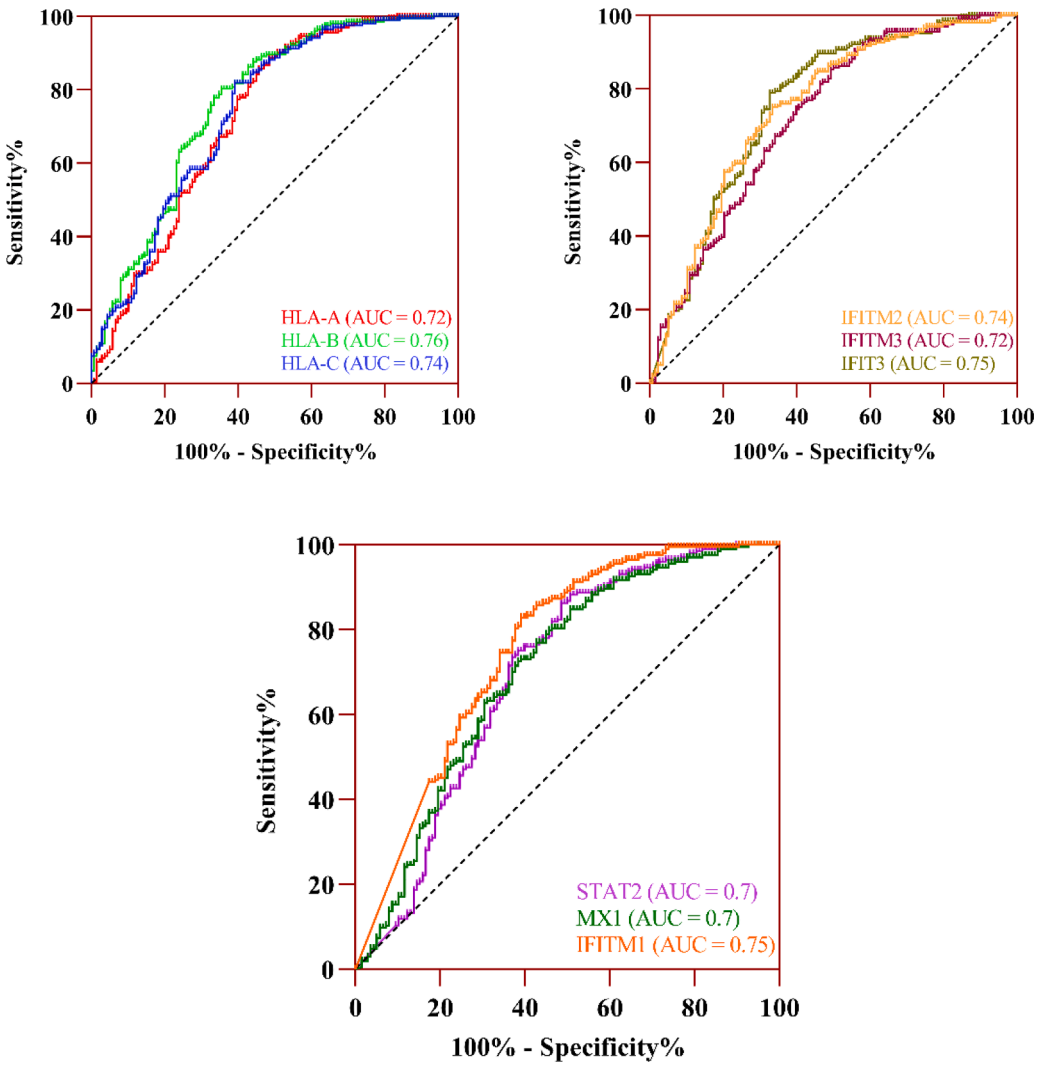

Fig. 12. Evaluation of the hub genes. ROC curves for 9 hub genes (HLA-A, HLA-B, HLA-C, IFITM2, IFITM3, IFIT3, STAT2, MX1 and IFITM1). The computed AUC area under the curve for dataset ranged from 0.7 to 1.

anaphylatoxin produced during induction of the complement system.

Our analyses also revealed down-regulation of a number of lncRNAs such as NEAT1 and CYTOR and up-regulation of AJUBA-DT, FALEC, MZF1-AS1, RNF139-DT, LMO7DN and SNHG31 lncRNAs. NEAT1 has been found to modulate innate immune responses during viral infections [18]. CYTOR is a tumor-associated lncRNA that can modulate inflammatory responses via epigenetic modifications [19].

GOE analysis of differentially expressed genes showed response to virus, cytokine-mediated signaling pathway, positive regulation of response to external stimulus and secretory granule membrane as the most important biological pathways enriched by these genes. Moreover, gene-concept network showed the importance of cytokine-mediated signaling pathway, positive regulation of response to external stimuli, response to polysaccharides, response to molecules of bacterial origin and response to virus in this condition.

Finally, the PPI network of DEGs showed the presence of a number immune-related genes such as those coding for HLA molecules and interferon regulatory factors among hub genes with the highest degree of connectivity.

Taken together, the *in silico* approach used in the current study highlights the importance of immune-related genes and pathways in the pathogenesis of COVID-19 and suggests novel targets for treatment of this disorder.

Declarations

Ethics approval and consent to participant:

Not applicable.

Consent of publication:

Not applicable.

Availability of data and materials:

The analyzed data sets generated during the study are available from the corresponding author on reasonable request.

Funding:

Not applicable.

Declaration of Competing Interest

The authors declare that they have no known competing financial interests or personal relationships that could have appeared to influence the work reported in this paper.

Data availability

Data will be made available on request.

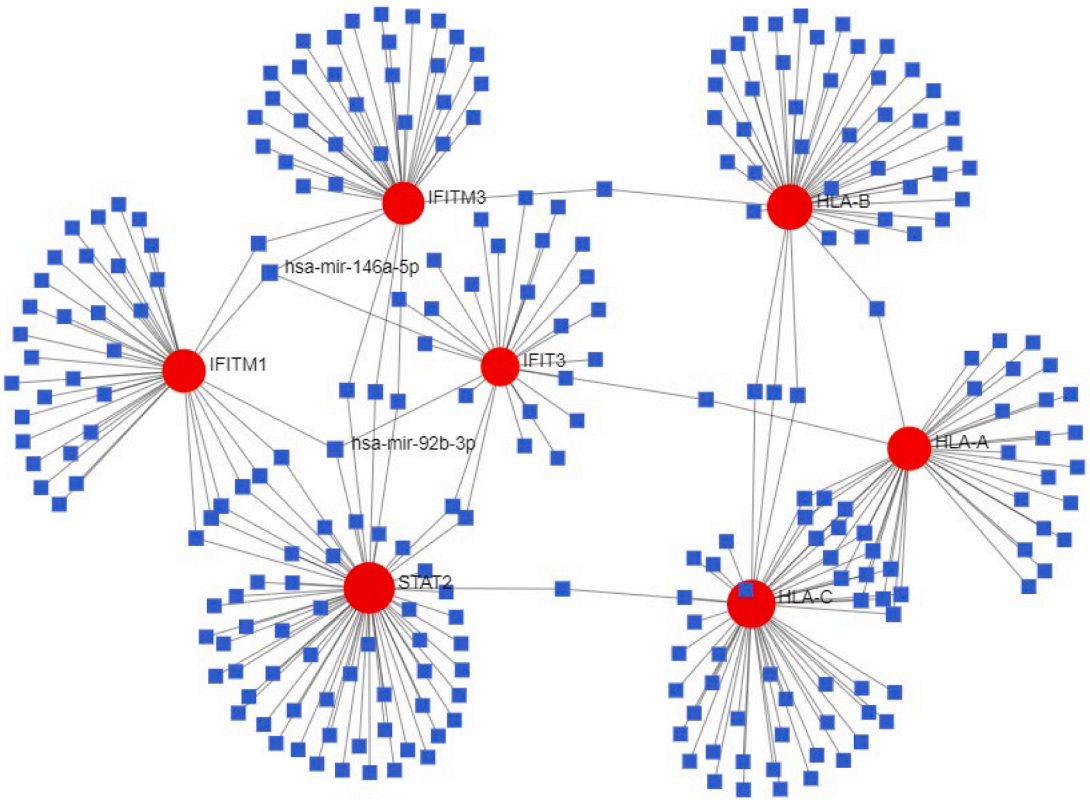

Fig. 13. The network of miRNA-hub genes. Circles represent the hub gene, while the squares represent miRNAs targeting the hub genes.

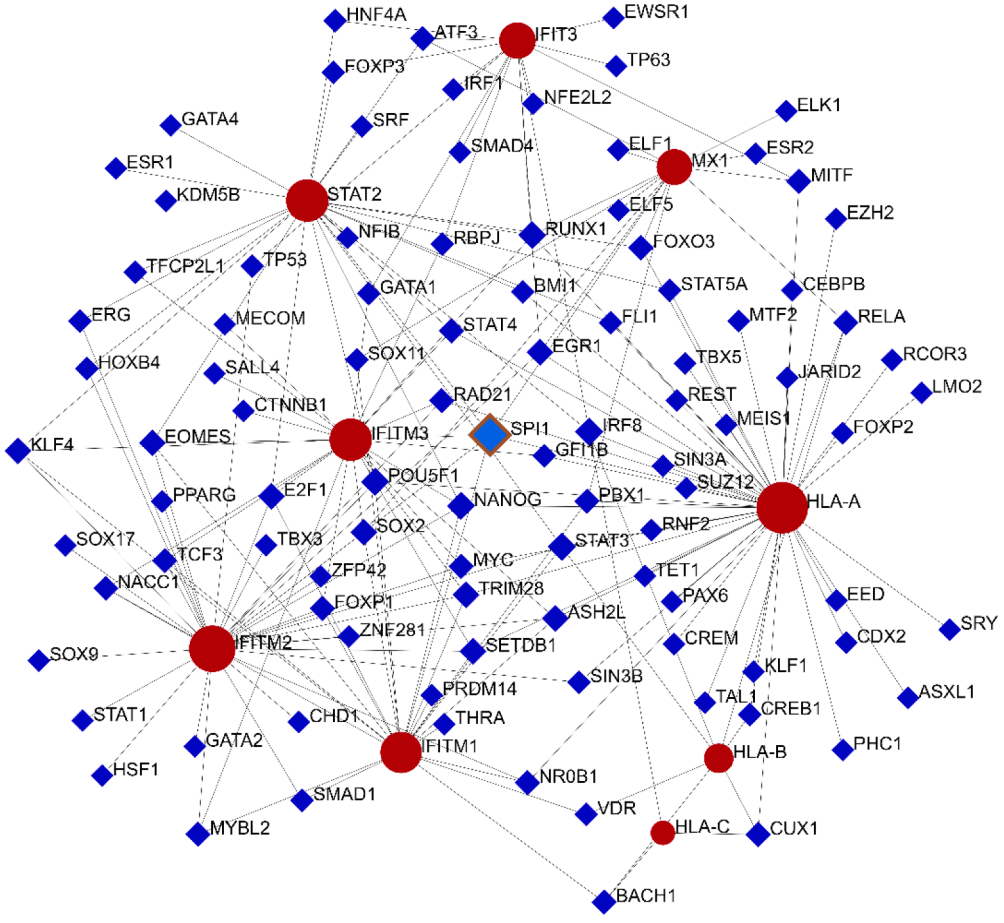

Fig. 14. The network of TF-hub genes. Circles show the hub gene, while the diamonds represent TFs targeting the hub genes.

Acknowledgement

The authors would like to thank the clinical Research Development Unit (CRDU) of Loghman Hakim Hospital, Shahid Beheshti University of Medical Sciences, Tehran, Iran for their support, cooperation and assistance throughout the period of study.

References

[1] M. Taheri, L.M. Rad, B.M. Hussen, F. Nicknafs, A. Sayad, S. Ghafouri-Fard, Evaluation of expression of VDR-associated lncRNAs in COVID-19 patients, BMC Infect. Dis. 21(1) (2021 Jun 19) 588. PubMed PMID: 34147082. Pubmed Central PMCID: PMC8214050. Epub 2021/06/2eng.

[2] M. Samsami, A. Fatemi, R. Jalili Khoshnoud, K. Kohansal, B.M. Hussen, S. Soghala et al., Abnormal transcript levels of cytokines among Iranian COVID-19 patients, J. Mol. Neurosci. MN. 72(1) (2022 Jan) 27–36. PubMed PMID: 34855144. Pubmed Central PMCID: PMC8636578. Epub 2021/12/03. eng.

[3] R. Wargodsky, P. Dela Cruz, J. LaFleur, D. Yamane, J.S. Kim, I. Benjenk et al., RNA Sequencing in COVID-19 patients identifies neutrophil activation biomarkers as a promising diagnostic platform for infections, Plos One 17(1) (2022) e0261679. PubMed PMID: 35081105. Pubmed Central PMCID: PMC8791486 diagnostics company developing RNA biomarkers for various diseases, including coronary artery disease and internal infections. TM is seeking patent protection for technology related to the current studies. This does not alter our adherence to PLOS ONE policies on sharing data and materials. The other authors declare there are no competing interests. Epub 2022/01/27. eng.

[4] A. Bass, Y. Liu, S. Dakshanamurthy, Single-cell and bulk RNASeq profiling of COVID-19 patients reveal immune and inflammatory mechanisms of infection-induced organ damage. Viruses 13(12) (2021 Dec 2) PubMed PMID: 34960687. Pubmed Central PMCID: PMC8706409. Epub 2021/12/29. eng.

[5] A.R. Daamen, P. Bachali, K.A. Owen, K.M. Kingsmore, E.L. Hubbard, A.C. Labonte et al., Comprehensive transcriptomic analysis of COVID-19 blood, lung, and airway, Sci. Rep. 11(1) (2021 Mar 29) 7052. PubMed PMID: 33782412. Pubmed Central PMCID: PMC8007747. Epub 2021/03/31. eng.

[6] M.I. Love, W. Huber, S. Anders, Moderated estimation of fold change and dispersion for RNA-seq data with DESeq2, Genome Biol. 15 (12) (2014) 550, 2014/12/05.

[7] T. Wu, E. Hu, S. Xu, M. Chen, P. Guo, Z. Dai, et al. clusterProfiler 4.0: A universal enrichment tool for interpreting omics data, Innovation (Camb) 2(3) (2021 Aug 28) 100141. PubMed PMID: 34557778. Pubmed Central PMCID: PMC8454663. Epub 20210701. eng.

[8] M. Kanehisa, S. Goto, KEGG: kyoto encyclopedia of genes and genomes. Nucleic Acids Res. 28(1) (2000 Jan 1) 27–30. PubMed PMID: 10592173. Pubmed Central PMCID: PMC102409. eng.

[9] D. Szklarczyk, A. Franceschini, S. Wyder, K. Forslund, D. Heller, J. Huerta-Cepas et al., STRING v10: protein-protein interaction networks, integrated over the tree of life. Nucleic Acids Res. 43(Database issue) (2015 Jan) D447-52. PubMed PMID: 25352553. Pubmed Central PMCID: PMC4383874. Epub 20141028. eng.

[10] P. Shannon, A. Markiel, O. Ozier, N.S. Baliga, J.T. Wang, D,. Ramage et al., Cytoscape: a software environment for integrated models of biomolecular interaction networks. Genome Res. 13(11) (2003 Nov) 2498–2504. PubMed PMID: 14597658. Pubmed Central PMCID: PMC403769. eng.

[11] C.-H. Chin, S.-H. Chen, H.-H. Wu, C.-W. Ho, M.-T. Ko, C.-Y. Lin, cytoHubba: identifying hub objects and sub-networks from complex interactome, BMC Syst. Biol. 8 (4) (2014) S11, 2014/12/08.

[12] G. Zhou, O. Soufan, J. Ewald, R.E.W. Hancock, N. Basu, J. Xia, NetworkAnalyst 3.0: a visual analytics platform for comprehensive gene expression profiling and meta-analysis, Nucleic Acids Res. 47(W1) (2019 Jul 2) W234–W241. PubMed PMID: 30931480. Pubmed Central PMCID: PMC6602507. eng.

[13] W. Luo, C. Brouwer, Pathview: an R/Bioconductor package for pathway-based data integration and visualization 29 (2013) 1830–1831. PMID.

[14] W. Luo, M.S. Friedman, K. Shedden, K.D. Hankenson, P.J. Woolf, GAGE: generally applicable gene set enrichment for pathway analysis, BMC Bioinform. 10 (1) (2009) 1–17.

[15] M. Kanehisa, S. Goto, KEGG: kyoto encyclopedia of genes and genomes, Nucleic Acids Res. 28 (1) (2000) 27–30.

[16] M. Kanehisa, M. Furumichi, Y. Sato, M. Ishiguro-Watanabe, M. Tanabe, KEGG: integrating viruses and cellular organisms, Nucleic Acids Res. 49 (D1) (2021) D545–D551.

[17] J. Melchjorsen, L.N. Sørensen, S.R. Paludan, Expression and function of chemokines during viral infections: from molecular mechanisms to in vivo function, J. Leukocyte Biol. 74 (3) (2003) 331–343.

[18] H. Ma, P. Han, W. Ye, H. Chen, X. Zheng, L. Cheng et al., The long noncoding RNA NEAT1 exerts antihantaviral effects by acting as positive feedback for RIG-I signaling. J. Virol. 91(9) (2017 May 1) PubMed PMID: 28202761. Pubmed Central PMCID: PMC5391460. Epub 2017/02/17. eng.

[19] C. Ou, X. He, Y. Liu, X. Zhang, lncRNA cytoskeleton regulator RNA (CYTOR): diverse functions in metabolism, inflammation and tumorigenesis, and potential applications in precision oncology, Genes Dis. (2021).